GEOREFERENCING AND RECTIFICATION OF SMARTPHONE IMAGES USING UAV REFERENCE IMAGES FOR MONITORING INFRASTRUCTURE CLOSE TO A RIVER

Hwiyoung Kim, Kyoungah Choi, Impyeong Lee
Lab. for Sensor & Modeling, Department of Geoinformatics, University of Seoul,
Seoulsiripdaero 163, Dongdaemun-gu, Seoul 02504, Korea,
Email: huddy@uos.ac.kr, shale@uos.ac.kr, iplee@uos.ac.kr

KEY WORDS: georeferencing, smartphone, UAV, reference images, infrastructure

ABSTRACT: The time and cost for recovering damaged infrastructure close to a river after disaster like typhoon, heavy rain and earthquake are increasing. It is thus important to monitor the infrastructure for maintenance and damage assessment effectively, particularly using remote sensors such as cameras. If we utilize smartphone images for monitoring the infrastructure, we can save significantly the time and cost to acquire up-to-date images. In this study, we develop a method to process smartphone images for infrastructure monitoring, using accurately pre-processed Unmanned Aerial Vehicles (UAV) reference images. First, we perform georeferencing of smartphone images based on their correspondence with UAV reference images. Then we project these georeferenced images onto target object surfaces. In this process, we derive the camera position and orientation for each smartphone image and the 3D coordinates of main object points appearing in smartphone images. We then verified the results by comparing them to surveyed reference data. It shows that we can utilize the rectified smartphone images to find the locations, length of cracks and areas of damaged structures. The proposed approach shows that smartphone images can be successfully used to monitor the damaged infrastructure close to a river.

1. INTRODUCTION

Recently the unexpected disasters like typhoons, heavy rains and earthquakes are occurring due to global warming resulted from a reckless destruction of nature mostly by humans. As a result, economical and human damages rapidly increase. In Korea, from 2005 to 2014, heavy rains happened 89 times with the greatest intensity of 25 in August during those 10-year period. Those heavy rains caused the death of 51 people and the loss of about 557.7 billion won (MPSS, 2016). Typhoons occurred 228 times during the corresponding period, particularly in August, occurred 8 times. The typhoons in August during the mentioned above period brought the death of 14 people and the loss of about 864.1 billion won (MPSS, 2016).

According to the disaster report 2014 from MPSS, disasters such as heavy rains, heavy snows and typhoons caused property damage estimated of 180 billion won. Public facilities accounted for 79.4%, about 142.9 billion won of the damage. Particularly the type of facilities classified as the infrastructure close to a river, which is dam, bridge and embankment, constituted 44%(about 62.8 billion won), 13.3%(about 19 billion won) and 2.7%(about 3.9 billion won) respectively. These types accounted for about 60% of public facilities (MPSS, 2015). This shows how important it is to monitor infrastructure close to a river. Unfortunately, the infrastructure is difficult to reach for people. This creates the opportunity to solve this problem by using data obtained from Unmanned Aerial Vehicles (UAV).

Tokmakidis and Scarlots (Tokmakidis and Scarlatos, 2002) used mini unmanned helicopter with a semi metric camera attached to its body to acquire images of an archeological site at the altitude of 30~40m, Digital Terrain Model (DTM) was created by using the images. Kumar et al (Kumar et al., 2013) utilized UAV with on-board navigation, guidance and control systems for automated aerial inspection of India's tallest tower, the 300m RCC tower (Kumar et al., 2013). Électricité de France (EDF; Electricity of France) mapped power lines to know the locations where the vegetation needs to be cut (Delair-Tech SAS, 2014). The altitude of flying was 150m and spatial resolution was about 3cm.

Though images of infrastructure reaching difficult for people can be acquired using UAV, georeferencing should be performed to monitor infrastructure. There are researches to perform georeferencing using sensed images for saving the time and cost of georeferencing. Wong and Clausi (Wong and Clausi, 2007) proposed a system to register satellite and aerial remotely sensed images obtained at different times or from different sensors. To complement the lack of direct georeferencing and relief displacement of single image, Oh et al. (Oh et al., 2010) used high-resolution stereo satellite imagery as a ground control source. Turner (Turner et al., 2012) presented a method of rectification and mosaicking of UAV images based on feature matching and Structure from Motion (SfM) point clouds created by estimated camera positions or ground control points (GCP).

These studies suggest some approaches of monitoring facilities using UAV and reference images. However these approaches have limitations for continuous monitoring. An equipment like UAV needs users to be skillful and is hard to operate at all times. What is more, the side of facilities is not visible on satellite images, which makes it difficult to use as reference images. These problems can be solved by combining smartphone and UAV images. First of them are easy to utilize and carry on, while the second one can be used as a reference data of the side of facilities.

This paper is constructed as follows. The methodology for georeferencing and rectification of smartphone images based on reference images will be presented and explained in Section 2 along with the proposed algorithm. The experimental result using the mentioned method is showed in Section 3, e.g. accuracy or result figure. Finally, conclusions are drawn based on the results in Section 4.

2. METHODOLOGY

In this study, we describe a methodology for geometric image correction of smartphone images. First, we define what UAV reference images are and explain why these images are used in the proposed algorithm. Secondly we perform Bundle Block Adjustment (BBA) based on reference images to georeference smartphone images acquired in random locations. At this stage, the accurately estimated position and orientation (Exterior Orientation Parameters, EOP) of smartphone images is obtained. Then we project the smartphone images onto target object surfaces using EOP of the images acquired through BBA. The flowchart of proposed method is represented in Figure 1.

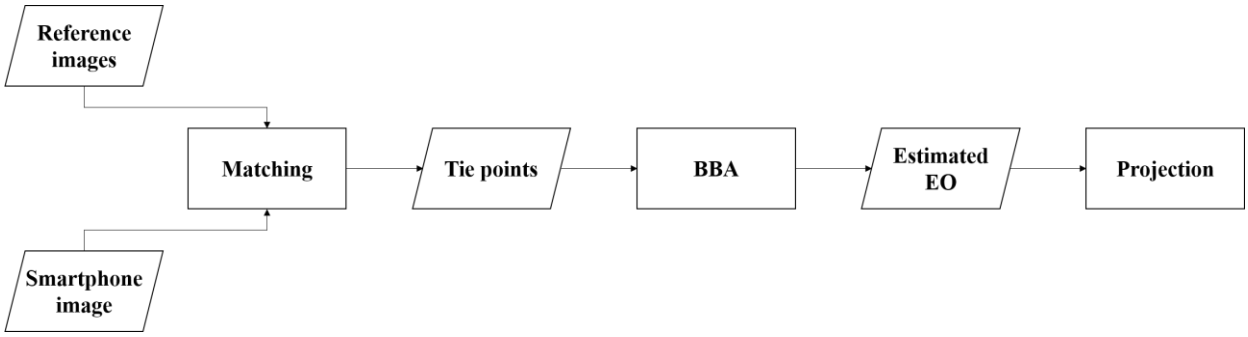

Figure 1. Flowchart of proposed method for georeferencing and rectification of smartphone images based on reference images

2.1 UAV Reference Images

Reference Images mean the images the accurately processed in advance. These images contain ground coordinates corresponding to a pixel coordinates, EOP of images and calibrated internal orientation parameters (IOP). They are accurately adjusted using GCP. The reason why UAV images are used as reference images is due to characteristic of infrastructure close to a river and UAV. The infrastructure is for people hard to reach, but UAV can approach the place for people hard to reach closely.

It is important to measure GCP to perform georeferencing of images accurately. In order to obtain GCP, the equipment like Global Navigation Satellite System (GNSS) receiver and Total Station is needed and people should go the surveying site. Therefore the time and cost for measuring GCP is huge. Alternatively we can obtain GCP through reference image without going to the site. In addition, the information about the accurate EOP and IOP of reference images can help to perform georeferencing of smartphone images. By using these elements, the error in perspective model like distortion can be minimized and the result can be estimated accurately.

2.2 BBA based on Reference Images

Georeferencing is performed to determine EOP of images. We use BBA as the method of georeferencing. BBA is based on collinearity equations where perspective center of the image, one ground point and the image point corresponding the ground point are collinear. Figure 2 shows the geometric relation of perspective center, image point and ground point.

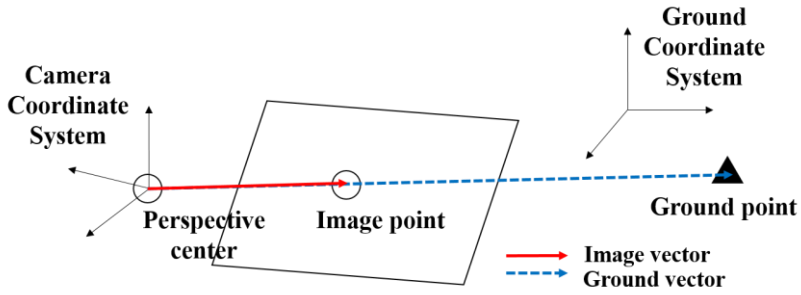

Figure 2. Conceptual diagram of collinearity equations

In this study, we perform georeferencing using reference images instead of GCP. It means BBA in this study is performed only based on tie points between reference and smartphone images and EOP of reference images. Though it is originally important to use GCP to estimate accurate EOP of images, UAV reference images can act as GCP. IOP of the reference images can reduce distortion of perspective model and EOP of them enables smartphone images to be adjusted accurately.

In order to perform BBA we need the initial EOP of smartphone images. Because collinearity equations are non-linear, it needs iterative solution. We can derive the initial value of smartphone images using at least four tie points between reference and smartphone images. Then we set EOP of reference images as constraint condition because we use reference images as control parameters (Choi and Lee, 2009). We can also determine initial value of ground points corresponding to the tie points.

2.3 Projection onto Target Surfaces

To utilize smartphone images for monitoring the infrastructure close to a river, they should be geometrically rectified. Geometric rectification in this study means projecting the image onto target object surfaces. The projection is also based on collinearity equations. We can obtain ground coverage of smartphone images projected onto target surface on reference images. Then we can resample pixels of the image performing back-projection. Figure 3 shows the illustration of projection onto target surfaces.

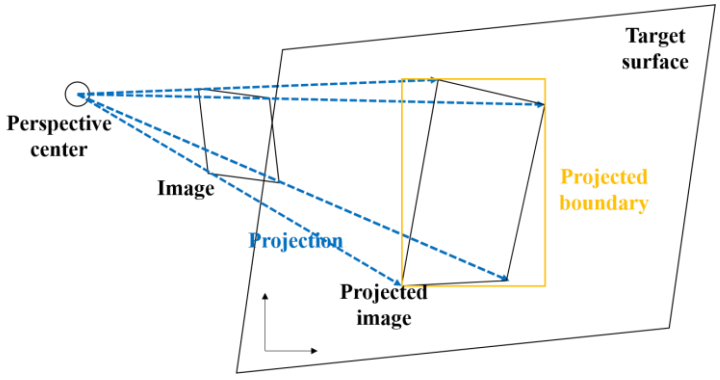

Figure 3. Conceptual diagram of projection onto the target surface

In addition to collinearity equations, if we have more than two lines for a tie point we can calculate the ground coordinate of the point. However it is possible to derive the ground coordinate using only one line because we define specific target plane. The only unknown parameter in Equation (1) is scale (λ). The scale can be derived through an intersection point between a collinear line and a plane. Equation (1) presents the collinearity condition and Equation (2) shows plane conditions.

$$P_C = \frac{1}{\lambda} R_{GC}(P_G - C_G) \tag{1}$$

where P_C: the image point in Camera Coordinate Systems (CCS)
λ: the ratio of length between image and ground

R_{GC}: the rotation matrix converting Ground Coordinate Systems (GCS) to CCS
P_G: the ground point in GCS
C_G: the perspective center in GCS

$$n^T p = d \tag{2}$$

where n: the normal vector of a plane
p: a point on the plane
d: the value of a point calculated by plane equations

We can derive the scale using Equation (3) as p in Equation (2) corresponds to P_G in Equation (1). Equation (3) represents the process of deriving the scale. As shown in Equation (4), ground coordinates of the projected image can be obtained.

$$\begin{aligned} n^T(\lambda R_{CG} P_C + C_G) &= d \\ \lambda n^T R_{CG} P_C &= d - n^T C_G \\ \lambda &= \frac{d - n^T C_G}{n^T R_{CG} P_C} \end{aligned} \tag{3}$$

where R_{CG}: the rotation matrix converting CCS to GCS

$$\begin{aligned} P_G &= \lambda R_{CG} P_C + C_G \\ P_G &= \frac{d - n^T C_G}{n^T R_{CG} P_C} R_{CG} P_C + C_G \end{aligned} \tag{4}$$

After calculating ground coordinates of the projected image, we can make a ground boundary of projected one. In order to create the boundary we need to define new coordinate system corresponding to the plane. Because the image are projected onto a common plane, there is no information about the coordinate axis creating a grid. The axis can be defined using the projected ground point. We can set first axis as the vector between one projected ground point and the other one. Second axis can be gained outer product of the normal vector of the plane and the vector used as first axis. These axes should be normalized.

The ground boundary of new coordinate system is converted to the one of ground coordinate system, then we perform back-projection of the ground boundary and pixels of the image are resampled. Finally the images are geometrically rectified and reconstructed through back-projection.

3. EXPERIMENTAL RESULT

3.1 Data Acquisition

In order to perform georeferencing and rectification of smartphone images, we acquired experimental data in Gangjeong-goryeong-bo (reservoir), Daegu, Korea. Table 1 presents the specification of UAV used in obtaining reference images and Table 2 shows the test data specification of UAV reference and smartphone images used in this tests.

The length of data acquisition section for UAV reference images was about 350m and the distance between UAV and the target infrastructure was about 87.3m. Smartphone images were obtained from two spots. One is under the infrastructure and the other is at the entrance of it. Figure 4 shows the test area, UAV reference and smartphone images. UAV reference images were collected in February 2016 and smartphone images in August 2016.

Table 1. UAV specification

Classification	Model	Dimensions	Payload	Flight time	Cruising speed
Specification	MD4-1000	113cm x 113m x 50cm	~1,200g	~90min	~12m/s

Table 2. Test data specification

Data	Site	Date	Focal length	Image resolution	Pixel size
UAV reference	Daegu, Korea	Feb 2016	35mm	6000x4000	6um
smartphone	Daegu, Korea	Aug 2016	3.85mm	4160x2340	1.25um

(a) (b) (c)

Figure 4. (a) Test area (b) UAV image (c) smartphone images

We can verify the accuracy of UAV reference images through Root Mean Square Error (RMSE) of check points. Table 3 shows check points RMSE of each axis. We used a set of 55 images as reference one and set the number of GCP as 43 and the number of check points as 18. About 10 points were used for each image with accuracy set to 5cm. The check points RMSE is about 10 cm.

Table 3. Check points RMSE of reference images with GCP

X error (cm)	Y error (cm)	Z error (cm)	XY error (cm)	Total (cm)
6.753	5.138	5.874	8.485	10.32

3.2 Georeferencing of Smartphone Images

In this study we do not use GCP to perform georeferencing of the smartphone images. We perform georeferencing only based on reference images. That is why we use estimated EOP and calibrated IOP of reference images determined in the previous step and set the accuracy of reference images with high-level accuracy as 0.01m, 0.01° because we assume the estimated EOP of reference images is true value.

To check the accuracy of EOP, we conducted experiment using the assumed true EOP of reference images. We set initial EOP of reference images as the true one with high-level accuracy and IOP of reference images as the calibrated one. Table 4 presents check points RMSE of the experiment. It shows the similar results with the test using GCP.

Table 4. Check points RMSE of reference images without GCP

X error (cm)	Y error (cm)	Z error (cm)	XY error (cm)	Total (cm)
6.215	6.704	5.902	9.141	10.881

The true value of EOP is needed for accuracy assessment of experimental results. Therefore we performed georeferencing using GCP to acquire true EOP. Table 5 presents true EOP of smartphone images and Table 6 shows the accuracy of the dataset of reference and smartphone images. We used calibrated IOP of reference images. As shown in Table 6, the accuracy of reference and smartphone images was worse. It could be considered that the geometric relation with reference and smartphone images is hard to match.

Table 5. True EOP of smartphone images

	X (m)	Y (m)	Z (m)	ω (°)	ϕ (°)	κ (°)
1	151444.875	360604.331	50.714	115.539	27.359	-15.971
2	151471.071	360630.425	58.388	-43.212	74.543	132.629
3	151401.760	360567.251	47.890	153.751	51.734	-53.608
4	151404.146	360568.561	49.772	110.923	-1.428	-4.797
5	151414.142	360578.493	49.975	115.962	2.177	-5.929
	⋮	⋮	⋮	⋮	⋮	⋮
12	151474.812	360627.745	58.547	5.012	75.875	80.613

Table 6. Check points RMSE of the true dataset

X error (cm)	Y error (cm)	Z error (cm)	XY error (cm)	Total (cm)
9.262	31.637	7.051	32.964	33.71

We performed three types of georeferencing approach to verify possible conditions and the accuracy of georefencing. First is georeferencing of reference and smartphone images without matching points, second approach is with matching points and third uses initial EOP of smartphone images instead of matching points. First method had no results for smartphone georeferencing. Matching is only performed in UAV images.

Second provided georeferencing results as EOP of smartphone images. This was possible because the matching points established the relative relation of reference and smartphone images. Table 7 presents EOP RMSE and Table 8 presents check points RMSE. EOP position RMSE is about 1m, orientation RMSE is from 4° to 8° and check points RMSE is about 62cm. These results are worse than the dataset with GCP. It could be considered that IOP of smartphone images from the dataset with GCP isn't correct.

Table 7. EOP RMSE between true and estimated value

	X (m)	Y (m)	Z (m)	ω (°)	ϕ (°)	κ (°)
RMS	0.854	1.337	0.646	8.377	4.657	6.726

Table 8. Check points RMSE of second approach

X error (cm)	Y error (cm)	Z error (cm)	XY error (cm)	Total (cm)
23.147	56.779	9.429	61.316	62.037

Third approach had no georeferencing results like First. Though we constrained the matching area by giving the initial EOP of smartphone images, the geometric relation between reference and smartphone images isn't established. Because the texture of reference and smartphone images is repeated continually, it is hard to establish the relationship between reference and smartphone images.

3.3 Rectification of Smartphone Images

In the process of georeferencing we obtained the EOP of smartphone images. According to the method of rectification mentioned above, we rectified the smartphone images to target surfaces using the EOP. Figure 5 presents the original smartphone image (a), the rectified image (b) and sections of surveying (c). The smartphone image is obtained as 5mm spatial resolutions.

(a) (b) (c)

Figure 5. (a) An original smartphone image (b) the rectified image (c) sections of surveying

We measured the length of a part of the infrastructure close to a river like a railing. The length of sections (1), (2) measured through the rectified image are 29.4cm, 95.1cm and through survey are 30.6cm, 92.4cm respectively. The difference of results measured through rectified image and survey is from about 1cm to 3cm. Considering the resolution of the smartphone image, this result didn't show the value satisfying it.

4. CONCLUSIONS

In this study, we proposed a method of georeferencing and rectification of smartphone images based on UAV reference images for monitoring the infrastructure close to a river. We acquired smartphone images, processed them based on UAV reference images. We analyzed the processing results comparing to the dataset processed with GCP. Then we obtained the rectified smartphone images.

Experimental results show that if there are no explicit matching points, even though there are the initial EOP, the georeferencing results aren't created. The accuracy is lower than one of UAV reference images even in the case that the georeferencing was performed. To improve the accuracy, the geometric relation of reference and smartphone images should be rectified and the problem resulted from their iterative patterns also be developed. If the problems are advanced, smartphone images can be utilized for continuous monitoring because they can save the cost of human and time.

ACKNOWLEDGMENTS

This research was supported by a grant (14SCIP-B065985-02) from Smart Civil Infrastructure Research Program funded by Ministry of Land, Infrastructure and Transport (MOLIT) of Korea government and Korea Agency for Infrastructure Technology Advancement (KAIA).

REFERENCES

Choi, K., Lee, I., 2009. Image Georeferencing using AT without GCPs for a UAV-based Low-Cost Multisensor System, Korea Society of Surveying, Geodesy, Photogrammetry and Cartography, 27(2), pp. 249-260.
Delair-Tech SAS, 2014. Power lines inspection using mini-uav, Delair-Tech, Madrid, Spain.
Kumar, K., Rasheed, A., Kumar, R., Giridharan, M., Ganesh, M., 2013. Dhaksha, the unmanned aircraft system in its new avatar-automated aerial inspection of India's tallest tower, International Archives of the Photogrammetry, Remote Sensing and Spatial Information Sciences, Volume XL-1/W2.
Ministry of Public Safety and Security, 2015. 2014 disaster chronology, Sejong, pp.69.
Ministry of Public Safety and Security, 2016. 2016 Analysis and prospect for disaster safety overall situation in August, Sejong.
Oh, J., Toth, C., Grejner-Brzezinska, D., 2010. Automatic georeferencing of aerial images using high-resolution stereo satellite images, ASPRS 2010 Annual Conference.
Tokmakidis, K., Scarlatos, D., 2002. Mapping excavations and archaeological sites using close range photos, International Archives of Photogrammetry Remote Sensing and Spatial Information Sciences, Corfu, September 2-6.
Turner, D., Lucieer, A., Watson, C., 2012. An automated technique for generating georectified mosaics from ultra-high resolution Unmanned Aerial Vehicle (UAV) imagery, based on Structure from Motion (SfM) point clouds, Remote Sensing, 4, 1392-1410.
Wong, A., Clausi, D., 2007, ARRSI: Automatic Registration of Remote-Sensing Images, IEEE Transactions on Geoscience and Remote Sensing, Vol. 45, No. 5, pp.1483-1493.